Original Article

JCBFM

Journal of Cerebral Blood Flow & Metabolism
2020, Vol. 40(6) 1338–1350

DOI: 10.1177/0271678X19865917
journals.sagepub.com/home/jcbfm
SAGE

Brain endothelial specific gene therapy improves experimental Sandhoff disease

Godwin Dogbevia[1,2,*], Hanna Grasshoff[1,*], Alaa Othman[1], Anke Penno[3] and Markus Schwaninger[1,*]

Abstract

In Tay-Sachs and Sandhoff disease, a deficiency of the lysosomal enzyme β-hexosaminidase causes GM2 and other gangliosides to accumulate in neurons and triggers neurodegeneration. Although the pathology centers on neurons, β-hexosaminidase is mainly expressed outside of neurons, suggesting that gene therapy of these diseases should target non-neuronal cells to reconstitute physiological conditions. Here, we tested in *Hexb*$^{-/-}$ mice, a model of Sandhoff disease, to determine whether endothelial expression of the genes for human β-hexosaminidase subunit A and B (*HEXA*, *HEXB*) is able to reduce disease symptoms and prolong survival of the affected mice. The brain endothelial selective vectors AAV-BR1-CAG-*HEXA* and AAV-BR1-CAG-*HEXB* transduced brain endothelial cells, which subsequently released β-hexosaminidase enzyme. *In vivo* intravenous administration of the gene vectors to adult and neonatal mice prolonged survival. They improved neurological function and reduced accumulation of the ganglioside GM2 and the glycolipid GA2 as well as astrocytic activation. Overall, the data demonstrate that endothelial cells are a suitable target for intravenous gene therapy of GM2 gangliosidoses and possibly other lysosomal storage disorders.

Keywords

AAV, endothelial cells, gene therapy, lysosomal storage disorder, Sandhoff disease

Received 13 March 2019; Revised 12 June 2019; Accepted 19 June 2019

Introduction

Lysosomal storage diseases form a heterogeneous group of inherited metabolic disorders in which metabolites accumulate due to a deficiency in lysosomal degradation. Overall, lysosomal storage diseases represent a major health problem, affecting about 1 in 4000–9000 newborns.[1] In the past few decades, enzyme replacement therapy has brought about a breakthrough in the treatment of patients with some of these disorders. The approach builds on the observation that cross-correction between cells is possible.[2] Cells deficient in lysosomal enzymes can be rescued by neighboring cells that express and secrete the missing enzyme. Enzymes are endocytosed and reach the lysosomes where they perform their tasks. Similarly, after intravenous administration, recombinant enzymes are taken up by cells in the liver, spleen, and other peripheral organs.

Unfortunately, it is difficult for recombinant enzymes to cross the blood–brain barrier. This poses a problem for treating cerebral lysosomal storage diseases such as the GM2 gangliosidoses Sandhoff disease and Tay-Sachs disease. GM2 gangliosidoses are caused by a deficiency in the lysosomal enzyme β-hexosaminidase A that degrades GM2. Pathogenic variants leading to Tay-Sachs disease are found in the gene for the α subunit (*HEXA*) of the dimeric enzyme, whereas in Sandhoff disease the gene of the β subunit is affected (*HEXB*).[3] In both diseases, GM2 ganglioside and GA2 glycolipid accumulate, resulting in a progressive loss of neurons and the development of neurological deficits.

[1]Institute for Experimental and Clinical Pharmacology and Toxicology, University of Lübeck, Lübeck, Germany
[2]Division of Cardiac Surgery, University of Ottawa Heart Institute, Ottawa, Canada
[3]Department of Cell Biology of Lipids, LIMES Institute, University of Bonn, Bonn, Germany
*These authors contributed equally to this work.

Corresponding author:
Markus Schwaninger, Institute for Experimental and Clinical Pharmacology and Toxicology, University of Lübeck, Ratzeburger Allee 160, 23562 Lübeck, Germany.
Email: markus.schwaninger@pharma.uni-luebeck.de

The life expectancy of affected individuals is shortened; children typically succumb to the infantile form of Sandhoff disease before the age of 5 years. No curative therapy is available so far.

To deliver β-hexosaminidase A across the blood–brain barrier, repeated intrathecal injections of the enzyme have been tested in experimental models.[4,5] Alternatively, the missing enzyme could be supplied to the brain by gene therapy. In a mouse model of Sandhoff disease (*Hexb*$^{-/-}$ mice), intracerebral injection of AAV-based gene vectors improved neurological symptoms and prolonged survival.[6] However, as GM2 gangliosidoses affect all parts of the CNS, up-scaling the therapy to the large human brain would require multiple intracerebral injections and might not be feasible due to the risk of infections and cerebral damage.[6] The blood supply could provide a noninvasive, alternative route to distribute gene vectors throughout the entire CNS. Indeed, vectors based on AAV serotype 9 cross the blood–brain barrier to some extent.[7] A high dose of AAV9 vector administered to *Hexb*$^{-/-}$ mice ameliorated the neurological deficit and prolonged survival but also triggered liver and lung tumors in many mice.[8] AAV has been associated with hepatocellular carcinoma due to insertional mutagenesis.[9] A new AAV9-based vector has apparently overcome this problem, however, and achieved an impressive prolongation of survival of *Hexb*$^{-/-}$ mice after intravenous injection.[10]

So far, gene therapeutic approaches have targeted neurons to express *HEXA* and *HEXB*. While this was successful in mice, cats, and sheep,[6,8,10–12] it led to neurodegeneration in nonhuman primates.[13] That primate neurons are particularly vulnerable to *HEXA*/*HEXB* overexpression in comparison to other species may be due to differences in GM2 metabolism.[14] Under physiological conditions, both subunits of β-hexosaminidase A are predominantly expressed in microglia and not in neurons[15,16] although GM2 gangliosides accumulate in neurons of patients with Tay-Sachs and Sandhoff disease.[17] These findings suggest a physiological cross-correction between microglia and neurons in the way that microglia supply β-hexosaminidase A activity to neurons. In line with this concept, the transgenic expression of *HEXB* in neurons prevented the neuronal accumulation of GM2 in *Hexb*$^{-/-}$ mice but had little effect on neuroinflammation.[18]

Assuming that non-neuronal expression of *HEXA*/*HEXB* represents the physiological situation and is required, at least in primates, for safe therapy of GM2 gangliosidoses, we attempted to direct the gene vector to non-neuronal cells in the CNS. As target we chose endothelial cells in the CNS, which are readily accessible from systemic circulation, form a stable non-proliferating cell population, and are able to release lysosomal enzymes.[19,20] Importantly, previous work has shown that transducing brain microcapillary endothelial cells provides a strategy for gene delivery and for treating lysosomal disorders.[21] We have developed a unique AAV vector (AAV-BR1) which, when systemically administered, is capable of transducing CNS endothelial cells and leading to a sustained gene expression.[22,23] Importantly, AAV-BR1 shows an unprecedented degree of selectivity for the CNS endothelium over other cell types, resulting in a favorable safety profile.[22,23] Here, we show that by intravenously injecting the AAV-BR1 vector for expressing human *HEXA* and *HEXB* in CNS endothelial cells of *Hexb*$^{-/-}$ mice, we were able to increase β-hexosaminidase A activity, decrease lysosomal storage of GM2 and GA2, and prolong survival.

Materials and methods

Animals

Hexb$^{-/-}$ mice (strain: B6; 129S4-Hexb^{tm1Rlp}/J, stock: 002914) were obtained from the Jackson Laboratory.[14] The mouse line was maintained by either crossing homozygous males with heterozygous females or by heterozygous matings under specific pathogen-free conditions. The *Hexb* genotype was determined by PCR of DNA isolated from ear clippings using the primers 5′- ATT TTA AAA TTC AGG CCT CGA-3′ (common), 5′ CAT AGC GTT GGC TAC CCG TGA-3′ (mutant), and 5′-CAT TCT GCA GCG GTG CAC GGC-3′ (wild-type). Animals were euthanized at the humane end point, indicated by significant weight loss, paralysis, or frequent seizure episodes. All mice were housed in individual, ventilated cages (IVCs) with 12-h light/dark cycles with food and water *ad libitum*. Mice were of both genders and 25–30 days old at the time point of vector injection. Their body weights were measured daily over 300 days. Brain, livers, and serum were extracted for analysis at the age of 110–120 days. Heterozygous or wild-type littermates (summarized as *Hexb*$^{+/?}$) or age-matched wild-type or heterozygous animals were used as controls. Investigators were blinded to treatment or genotype of mice, or both, in all experiments.

Plasmid constructs

The sequence encoding human hexosaminidase A (*HEXA*, accession numbers NM_000520.4) was amplified by PCR from human cDNA with the forward primer containing the sequence of an inserted restriction site of Bstb1, named hHexA_BstB_S (5′-CGA TTC GAA TTC ACC ATG ACA AGC TCC AGG C-3′), and a reverse primer containing the sequence of an inserted restriction site of Not1, named

hHexA_Not_AS (5′-GCT TGC GGC CGC TTT ATC AGG TCT GTT CAA A-3′). The 1.6-kb fragment was cloned into the vector pAAV-CAG-NEMO-2A-eGFP[23] by removing NEMO-2A-eGFP with BstB1 and Not1 and replacing it with *HEXA*, generating the plasmid pAAV-CAG-*HEXA*. Similarly, the sequence encoding human *HEXB* (with accession number NM_000521.3) was amplified from the plasmid HsCD00004511 (DNASU Plasmid Repository, Arizona State University), with the forward primer containing the sequence of an inserted restriction site of Bstb1, named hHexB_BstB_S (5′-CGA TTC GAA TTC ACC ATG GAG CTG TGC GGG C-3′), and the reverse primer containing the sequence of an inserted restriction site of Not1, named hHexB_Not_AS (5′-TTT GCG GCC GCT TTA TTA CAT GTT CTC ATG G-3′). The 1,668-bp *HEXB* fragment was inserted into the vector pAAV-CAG-NEMO-2A-eGFP by removing NEMO-2A-eGFP with BstB1 and Not1. The new plasmid was named pAAV-CAG-*HEXB*. The plasmid pAAV-CAG-Ø was generated by the restriction digest of pAAV-CAG-eGFP with Nco1 and Fse1 (to remove the eGFP), blunted, and religated. The resulting plasmid pAAV-CAG-Ø only contained the CAG promoter without a transgene.

Vector production and quantification

Recombinant AAV vectors were produced by triple transfection of HEK293T cells as previously described.[23] HEK293T cells were transfected with plasmid DNA by the calcium-phosphate method.[24] Three days after transfection, cells were harvested, lysed in TNT extraction buffer (20 ml 1 M Tris-HCl pH 7,5, 150 ml 1 M NaCl, 10 ml 1 M $MgCl_2$, 100 ml 10% triton X-100, and 720 ml water). The vectors were purified via affinity column purification using Hi Trap™ AVB sepharose ™, GE Healthcare. For transfections, we used p179 as adenoviral helper plasmid (Xiao X, Li J and Samulski RJ, 1998), the pAAV-CAG-*HEXA* and pAAV-CAG-*HEXB* (containing inverted terminal repeats of AAV2), and a plasmid encoding the AAV-BR1 capsid.[23,25] Genomic titers were determined by quantitative real-time PCR using the woodchuck (WRPE)-specific primers WPRE-F 5′-ACT GTG TTT GCT GAC GCA AC-3′ and WPRE-R 5′-CAA CAC CAC GGA ATT GTC AG-3′ for the plasmids pAAV-CAG-HEXA and pAAV-CAG-HEXB and CAG-specific primers CAG-internal-F (5′-AAC GCC AAT AGG GAC TTT C-3′) and CAG-internal-R (5′-GTA GGA AAG TCC CAT AAG GTC A-3′) for the plasmid pAAV-CAG-Ø.

To determine vector copy numbers, we used the SYBR Green I-based FastStart Essential DNA Green Master (Roche) with the Light Cycler Nano system (Roche) or the Platinum SYBR Green qPCR Supermix (Invitrogen) with the ABI Prism 7000 Sequence Detection system (Applied Biosystems). An initial denaturation of the probes (95 °C, 10 min) was followed by 45 cycles of amplification (95°C/67°C/72°C; 30 s each; rampage 5°C/s) and a final melting curve analysis (60°C to 97°C with 0.1°C/s). WPRE forward and reverse primers or CAG forward and reverse primers, as described above, were used for titration.

*Intravenous injection of AAV-BR1-CAG-*HEXA/B *and AAV-BR1-CAG- Ø into adult and neonatal mice*

Under anesthesia with 2.5% isoflurane and 97.5% oxygen 25- to 30-day-old $Hexb^{-/-}$ mice received an intravenous injection with AAV-BR1 vectors expressing either *HEXA* and *HEXB* or a control vector (AAV-BR1-CAG-Ø, 1.8×10^{11} gp/mouse in 100 µl) in the retroorbital venous sinus. This dose proved to be efficacious in previous studies.[22,23]

For the treatment of neonatal $Hexb^{-/-}$ mice with the vectors, AAV-BR1-CAG-*HEXA*/*B* and AAV-BR1-CAG-Ø were injected intravenously into the temporal vein using a stereo microscope. Owing to increased lethality and neurotoxicity of isoflurane, neonatal mice were not anesthetized. The $Hexb^{-/-}$ mice received 6.0×10^{10} gp/mouse of the vector AAV-BR1-CAG-Ø or 3.0×10^{10} gp/mouse of each AAV-BR1-CAG-*HEXA* and AAV-BR1-CAG-*HEXB* in a volume of 50 µl. Again, the dose was selected based on previous experience.[23]

Male and female mice were of similar age and weight and randomly allocated to vector treatment groups. Age-matched or littermate $Hexb^{+/+}$ or $Hexb^{+/-}$ (summarized as $Hexb^{+/?}$) served as controls.

Vector genome determination using qPCR

At the end of the survival experiment, total DNA was extracted from brain, liver, lung, and heart using the DNeasy tissue kit (Qiagen) according to the manufacturer's instructions. Extracted DNA was quantified using a spectral photometer (Nanodrop ND-2000C (Peqlab). AAV vector DNA in tissues was analyzed by qPCR using WPRE primers (5′-ACT GTG TTT GCT GAC GCA AC-3′ and 5′-CAA CAC CAC GGA ATT GTC AG-3′) or CAG-specific primers (5′-GGA CTC TGC ACC ATA ACA CAC-3′ and 5′-GTA GGA AAG TCC CAT AAG GTC A-3′) and Platinum SYBR Green qPCR Supermix (Invitrogen) with the ABI Prism 7000 Sequence Detection system (Applied Biosystems). Vector copy numbers were normalized to 100 ng total DNA.

RNA in situ hybridization using RNAscope

RNA *in situ* hybridization was performed using the commercially available RNAscope from Advanced

Cell Diagnostics (ACD). Probes for the human mRNA *HEXA* and *HEXB* that show no cross-reaction with the murine *Hexa* and *Hexb* mRNA was designed and was used in a fluorophore multiplex assay with three channels. *HEXB* was detected with fluorescein (1:1000), *HEXA* with cyanine 5 (dilution 1:1,000). *Pecam*, a marker for endothelial cells, was detected with cyanine 3 (dilution 1:1000). RNAscope was performed on 20-µm-thick brain sections of $Hexb^{+/+}$ and $Hexb^{-/-}$ mice that were intravenously treated with the vectors AAV-BR1-CAG-*HEXA*/B (total dose: 1.8×10^{11} gp/mouse). The brains were extracted 14 days after the injection. C57BL/6 mice that received no vector injection served as controls.

Infection of primary brain endothelial cells

Primary brain endothelial cells (PBECs) prepared from wild-type or $Hexb^{-/-}$ mice were cultured in 24-well plates as described previously.[26] Three days after preparation, cells were transduced with 1.0×10^{10} genomic particles/well of the vectors AAV-BR1-CAG-*HEXA*/*B*. Medium was changed five days after infection. Two days later, medium and cells were harvested and frozen at −20°C for later use.

Quantification of GM2

For lipid extraction, 250 µl of brain lysates (26 µg/µl protein) prepared as described below were mixed with 1 ml methanol (MeOH) and 0.75 ml $CHCl_3$/ MeOH/ H_2O (10/5/1) and then incubated in an ultrasonification bath for 5 min and at 37°C for 4 h. Samples were centrifuged at 1000 *g* for 5 min and the supernatant was transferred to a new tube. The pellet was re-extracted in the same manner with 2 ml $CHCl_3$/MeOH (1/1) and subsequently with 2 ml $CHCl_3$/MeOH (2/1). The three resulting supernatants were pooled and the solvents evaporated. Lipids were dissolved in 1 ml $CHCl_3$. The resulting lipid samples (100 µl, 0.65 mg protein) were placed on TLC silica plates (Merck, 1.05721.0001). Plates were developed in $CHCl_3$/triethylamine/EtOH/ H_2O (35/35/40/9), dried, sprayed with aqueous 20% sulfuric acid, and incubated at 160°C for 20 min. Plates were scanned (Powerlook 1100, UMAX) and the GM2 and sphingomyelin (SM) lipid bands were quantified (GelPro analyzer software, Media Cybernetics).

Liquid chromatography-mass spectrometry (LC/MS) for GM2 and GA2

Lipid extraction was performed as described previously[27] with some modifications. The internal standard d3-GM2(18:1/18:0) (40 pmol dissolved in 160 µl methanol) was added to 20 µl of brain lysate. Samples were continuously mixed in a thermomixer (Eppendorf) at 25°C (950 r/min, 30 min) to allow protein precipitation. After centrifugation for 10 min (16,000 *g*, 25°C) the single-phase supernatant was collected, dried in a SpeedVac, and stored at −20°C until analysis. Before analysis, the dried lipids were redissolved in 100 µl MeOH.

Liquid chromatography was done as described previously[28] with some modifications. The lipids were separated using C30 reverse-phase chromatography. Dionex Ultimate 3000 RS pump (Thermo Scientific) was used with the following mobile phases: A) acetonitrile:water (6:4) with 10 mM ammonium acetate and 0.1% formic acid and B) isopropanol: acetonitrile (9:1) with 10 mM ammonium acetate and 0.1% formic acid. The C30 Accucore LC column (Thermo Scientific) with the dimensions 150 mm × 2.1 mm × 2.6 µm was used. The following gradient was employed with a flow rate of 0.26 ml/min; 0.0–0.5 min (isocratic 30%B), 0.5–2 min (ramp 30–43% B), 2.10–12.0 min (ramp 43–55% B), 12.0–18.0 min (ramp 65–85%), 18.0–20.0 min (ramp 85–100% B), 20–35 min (isocratic 100%B), 35–35.5 min (ramp 100–30% B), and 35.5–38 min (isocratic 30% B).

The liquid chromatography was coupled to a hybrid quadrupole-orbitrap mass spectrometer (Q-Exactive, Thermo Scientific). Ionization was achieved using heated electrospray ionization with the following parameters: positive-mode voltage (3500 V), negative-mode voltage (3200 V), capillary temperature (300°C), sheath gas (40 arb unit), aux gas (10 arb units), and HESI probe temperature (320°C). A data-dependent acquisition with positive and negative polarity switching was used. We performed a full scan from 250–3000 m/z at a resolution of 70,000 and AGC target of $3e^6$ while data-dependent MS^2 scans (top 10) were acquired using normalized collision energies of 25 and 30 and a resolution of 17,500 and AGC target of $1e^5$. Lipids were identified by using four criteria: (1) high accuracy with a m/z shift of less than 5 ppm from the predicted value and a resolving power of 70,000 at 200 m/z (for GM2 (d36:1) (d18:1/18:0), [M+H]+ (m/z 1384.83111), and [M-H]- (m/z 1382.81546); for GA2 (d36:1) (d18:1/18:0), [M+H] m/z 1093.73569), and [M-H]- (m/z 1091.72004)); (2) isotopic pattern fitting to expected isotopic distribution; (3) retention time fitting to the internal standard; and (4) matching of the specific MS2 fragments (for both GM2 (d36:1) (d18:1/18:0) and GA2 (d36:1) (d18:1/18:0); in the positive mode m/z of 548.54011, 300.28971, 282.27914, 264.26858, 252.26858, and 60.04439 and in the negative mode 1091.72972, 564.5447, and 290.08814). Quantification was done using single-point calibration by comparing the area under the peak of each lipid species to the area under the peak of the internal standard. Then, these data were normalized to sample

protein content. With this procedure, we could identify GM2 and GA2 species. Data were analyzed by using Tracefinder and FreeStyle software (ThermoScientific).

Tissue and serum preparation for enzymatic assay and GM2 measurements

Prior to perfusion, blood samples were collected from the abdominal aorta of mice. Blood was allowed to clot at 4°C and then centrifuged at 2400 r/min for 15 min. The clear serum was collected and stored at −20°C. The mice were perfused with PBS and brain and liver were extracted on dry ice and frozen at −80°C. Tissues for enzymatic assays were homogenized in PBS supplemented with protease inhibitors (complete mini; Roche Diagnostic, Germany) and centrifuged at 11,000 r/min for 20 min. Supernatants were analyzed in assays.

Total β-hexosaminidase activity assay

Total β-hexosaminidase activity was measured in serum, brain, and liver lysates as well as in PBEC lysates and cell medium using the artificial substrate 4-methylumbelliferyl-2-acetamido-2-deoxy-β-D-glucopyranoside (4-MUG) (Melford Laboratories, UK) and an established protocol.[29] The generated fluorophore was measured at an emission wavelength of 440 nm after excitation at 365 nm using FLUOstar OPTIMA microplate reader (BMG Labtech, Germany).

Histology and microscopy

Mice were transcardially perfused with PBS and brains and livers extracted and frozen at −80°C. Cryosections of brains (20 µm) were prepared for staining. Tissues for immunostaining were fixed in MeOH for 10 min followed by washing in PBS and blocking in 1% BSA at room temperature for 30 min. Staining was done overnight with a primary rabbit anti-GFAP antibody (BD Pharmingen #557355), 1:500 dilution in blocking buffer. The following day, sections were washed three times in PBS and later incubated in a secondary anti rabbit Cy3 antibody, at a 1:400 dilution (Jackson/Dianova, #711-165-152) and 4′,6-diamidino-2-phenylindole (DAPI; 1 µg/ml) in blocking buffer for 2 h at room temperature. Sections were washed twice in PBS and mounted with Mowiol 4-88 containing 1,4-diazabicyclo-(2,2,2)octane, and coverslips for imaging. Three images per animal and brain region were analyzed. GFAP-positive cells with a DAPI-stained nucleus were counted.

Brain tissues for periodic acid–Schiff (PAS) staining (Sigma) were fixed as described above. PAS staining was performed according to the manufacturer's instructions. In brief, slides were oxidized in periodic acid solution for 5 min at room temperature, rinsed with distilled water, and immersed in Schiff's reagent (1:10 dilution with distilled water for 45 s). After washing the slides in running tap water for 5 min, the slides were counterstained with hematoxylin solution (1:100 dilution with distilled water for 30 sec). The slides were mounted using a toluene-xylene-based mounting medium (DPX Mountant, Sigma). Five images per animal and brain region were analyzed. PAS-positive spots were allocated to single cells according to nuclear staining.

Fluorescence and bright-field images were taken with a DMI 6000 B fluorescence microscope (Leica) with two objectives: HCXPL FLUOTAR 10.0x, aperture 0.3 and HCXPL FLUOTAR L 20.0x, aperture 0.4. A Leica DFC360FX camera was used for fluorescence images and a Leica DFC295 camera for bright-field images with the acquisition software LAS AF. Images were analyzed with ImageJ software. Images were not manipulated in any way except to adjust brightness and contrast. The final figures showing immunofluorescence images were assembled using the Illustrator (Adobe) software.

Rotorod and grip strength

We used the Rota-Rod for Mice of Ugo Basile (Italy; Cat. # 47600) for measuring the latency to fall off a rotating rod. The test was performed at a constant speed of 5 r/min for 300 s.

The grip strength was measured with the device of Ugo Basile (Italy; Cat. # 47200) according to the manufacturer's instructions. Each mouse had three chances to perform the tasks and the best performance was used for analysis. The rotarod test was performed once a week from the age of 39 days to the age of 154 days, the grip strength test was performed from the age of 78 days to the age of 148 days.

Statistics

Statistical analysis was performed using the GraphPad Prism software (GraphPad Software, San Diego, CA). If not indicated otherwise, data were tested for normality by D'Agostino & Pearson omnibus normality test and analyzed by unpaired t test, one-way ANOVA, or two-way ANOVA followed by Bonferroni's multiple comparison test (comparing all pairs of columns). Data are presented as mean ± SD. P values < 0.05 were considered statistically significant.

Study approval and reporting

All animal experiments were performed in accordance with the European Community Council Directive of November 24, 1986 (86/609/EEC) and the German

Animal Welfare Act. All efforts were made to minimize pain or discomfort of animals. Results are reported according to the ARRIVE guidelines. Animal experiments were approved by the ethics review board at the Ministerium für Energiewende, Landwirtschaft, Umwelt, Natur und Digitalisierung, Schleswig-Holstein, Germany.

Results

In vitro *and* in vivo *assessment of HEXA/HEXB expression*

To investigate the therapeutic effects of producing β-hexosaminidase A in CNS endothelial cells of $Hexb^{-/-}$ mice, we generated two CNS endothelial-selective AAV-BR1 vectors expressing the human hexosaminidase α subunit (AAV-BR1-CAG-*HEXA*) and human hexosaminidase β subunit (AAV-BR1-CAG-*HEXB*). A third vector expressing no gene of interest (AAV-BR1-CAG-Ø) served as control. To test the functionality of the vectors, primary brain endothelial cells (PBECs) prepared from $Hexb^{-/-}$ mice were transduced with AAV-BR1-CAG-*HEXA* and AAV-BR1-CAG-*HEXB,* each at a dose of 0.5×10^{10} genomic particles (gp) per pocket of a 24-well plate, while control pockets received 1.0×10^{10} gp of the vector AAV-BR1-CAG-Ø. Ten days post transduction, both supernatant and cell lysates were harvested for measuring total β-hexosaminidase activities by using the artificial substrate 4-MUG. Compared to the control, an 11-fold and 5-fold increase in β-hexosaminidase activity was observed in cell lysates and in supernatants of AAV-BR1-CAG-*HEXA*/*B* transduced cells, respectively ($p < 0.001$) (Figure 1(a)).

To evaluate brain transduction efficiency of the vectors *in vivo*, 25- to 30-day-old $Hexb^{-/-}$ mice received an intravenous injection of AAV-BR1-CAG-*HEXA*/*B* or the control vector AAV-BR1-CAG-Ø at a dose of 1.8×10^{11} gp per mouse. Two weeks post vector injections, brain and liver were harvested and lysed and the total β-hexosaminidase activities were determined (Figure 1(b)). While β-hexosaminidase activity increased significantly in brain lysates (Figure 1(b), $p < 0.0001$) of the AAV-BR1-CAG-*HEXA*/*B*-treated mice compared to the control, the activity in the liver did not change significantly (Figure 1(b), $p > 0.05$), indicating that the vector injected systemically transduced mainly cells in the CNS.

To evaluate the tissue distribution of the systemically administered vector, we determined the vector load in brain, liver, lung, and heart lysates by qPCR 80-85 days after injecting AAV-BR1-CAG-*HEXA*/*B*. Genomic vector particles were normalized to total tissue DNA. In brain lysates, we found significantly more genomic vector particles than in the other organs (Figure 1(c)), confirming the selectivity of the vector in targeting the brain.[23]

To localize the transduced human genes *HEXA* and *HEXB* in mouse brains, we performed *in situ* hybridization with probes that are specific for human *HEXA* and *HEXB* expressed through the vectors. In brain sections of $Hexb^{+/+}$ mice that received no vector injection, there was no signal for human *HEXA* or *HEXB* mRNA (data not shown). Therefore, we treated $Hexb^{+/+}$ and $Hexb^{-/-}$ mice with the vectors AAV-BR1-CAG-*HEXA*/*B* (1.8×10^{11} gp/mouse) at the age of 30 days. Two weeks after administering AAV-BR1-CAG-*HEXA* and AAV-BR1-CAG-*HEXB*, we observed signals for both human genes in cells that expressed *Pecam* as a marker of endothelial cells (Figure 1(d), Supplementary Figure 1). In summary, AAV-BR1-CAG-*HEXA*/*B* vectors transduce brain endothelial cells *in vitro* and *in vivo* and increase β-hexosaminidase activity.

Expression of HEXA/B *improves survival rates and motor activities in* $Hexb^{-/-}$ *mice*

$Hexb^{-/-}$ mice show no obvious phenotype in the first 80–90 days of their lives; however, there is a progressive neuronal damage, which leads to spastic movements of limbs, impaired coordination, tremors, muscle weakness, and, ultimately, death within 100–140 days.[14] To investigate whether CNS endothelial delivery of *HEXA*/*B* will improve motor activity and ultimately survival in these mice, we intravenously administered AAV-BR1-CAG-*HEXA*/*B* (each 3.0×10^{10} gp/mouse) or the control vector AAV-BR1-CAG-Ø (6.0×10^{10} gp/mouse) immediately after birth at P0/P1. The AAV-BR1-CAG-*HEXA*/*B*-treated group survived significantly longer and lost less body weight in the disease phase after day 90 (Supplementary Figure 2). To enhance the translational potential of the gene therapy, we wanted to test whether treatment at a later stage after genetic diagnosis has been performed would also be effective. Therefore, we treated two groups of 25- to 30-day-old $Hexb^{-/-}$ mice with either AAV-BR1-CAG-*HEXA*/B ($n = 19$) or the control vector ($n = 18$). Control vector-treated mice exhibited the disease phenotype within 80–90 days and reached a moribund end point at a median age of 130 days (survival range between 95 and 142 days, Figure 2(a)). $Hexb^{-/-}$ mice treated with AAV-BR1-CAG-*HEXA*/*B* had a longer life span with a median survival age of 189 days (survival range between 136 -> 300 days) (Figure 2(a), 2(b)).

To evaluate motor function in these mice, we performed rotarod and grip-strength experiments. In the rotarod setup, the latency to fall from a rod rotating with constant speed was investigated for 300 s starting

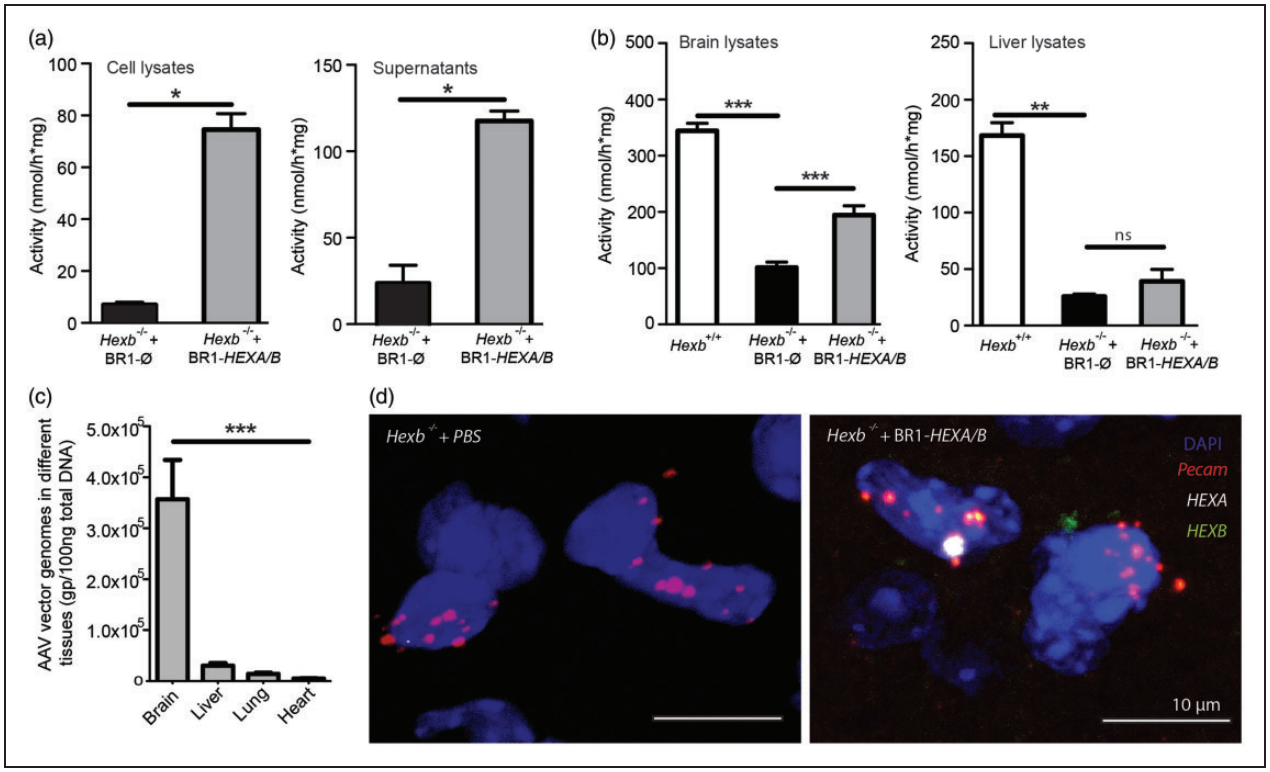

Figure 1. Effective transduction of brain endothelial cells for the release of β-hexosaminidase. (a) β-hexosaminidase activities were measured with the substrate 4-MUG in cell extracts and media from $Hexb^{-/-}$ primary brain endothelial cells that were transduced *in vitro* with AAV-BR1-CAG-*HEXA/B* or a control vector. There was a significant increase in β-hexosaminidase activity in the AAV-BR1-*HEXA/B*-transduced group compared to the control in the cell lysates and the supernatant. Data represent means ± SD. $*p < 0.05$ (*t* test, $n = 4$). (b) β-hexosaminidase activities in brain (left) and liver (right) lysates of $Hexb^{-/-}$ mice treated with AAV-BR1-*HEXA/B* and the control vector AAV-BR1-CAG-Ø. $Hexb^{+/+}$ animals served as controls. Data represent means ± SD. Brain, $F(2/14) = 128.1$ ($p < 0.0001$, one-way ANOVA); liver, $F(2/13) = 74.69$ ($p < 0.0001$, one-way ANOVA). $**p < 0.01$; $***p < 0.0001$ (Bonferroni test, $n = 5$ per group). (c) AAV genome copy number from different tissues indicates vector particles accumulated more in the brain than other organs. $Hexb^{-/-}$ mice received AAV-BR1-CAG-*HEXA* and AAV-BR1-CAG-*HEXB,* each in a dose of 3.0×10^{10} gp/mouse at P0/P1. Data are means ± SD. $F(3/143) = 12.86$ ($p < 0.0001$, one-way ANOVA). $***p < 0.0001$ (Bonferroni test, $n = 32$–48 per group) (d) *In situ* hybridization for human *HEXA* and *HEXB* mRNA revealed that the vectors AAV-BR1-CAG-*HEXA/B* transduced *Pecam*-positive brain endothelial cells.

at the age of 39 days up to the age of 154 days (Figure 2(c)). The performance of the control vector-treated mice deteriorated rapidly at the onset of the disease while the *HEXA/B*-treated mice performed better than the group treated with the control vector. In control $Hexb^{-/-}$ mice, impairment of coordination on the rotarod started around day 88. Although some of the AAV-BR1-CAG-*HEXA/B*-treated mice exhibited initial symptoms on the rotarod around day 102, at day 154, when the last rotarod test was performed, four out of eight surviving mice showed no impairment in the rotarod test. Overall, AAV-BR1-CAG-*HEXA/B*-treated mice outperformed the control group at every stage of the experiment.

To determine motor strength in the forearms, we performed grip-strength experiments from the age of 63 days up to the age of 148 days. In the grip-strength experiment, $Hexb^{-/-}$ mice that received the vector AAV-BR1-CAG-Ø first started to show impairment at the age of 80–90 days. Three out of eight surviving $Hexb^{-/-}$ mice treated with AAV-BR1-CAG-*HEXA/B* were still unimpaired at the age of 148 days when the experiment ended (Figure 2(d)).

Expression of HEXA/B *reduces GM2 ganglioside storage in the brain*

The increased survival rate and improved motor function in the AAV-BR1-CAG-*HEXA/B*-treated mice indicated efficacy of endothelial production and secretion of β-hexosaminidase. To assess its impact, we stained for ganglioside accumulation in the brain using the PAS reaction on fixed brain sections. No PAS-positive deposits were observed in wild-type control brain sections (Figure 3(a)). In $Hexb^{-/-}$ mice treated with the control vector, there were significantly

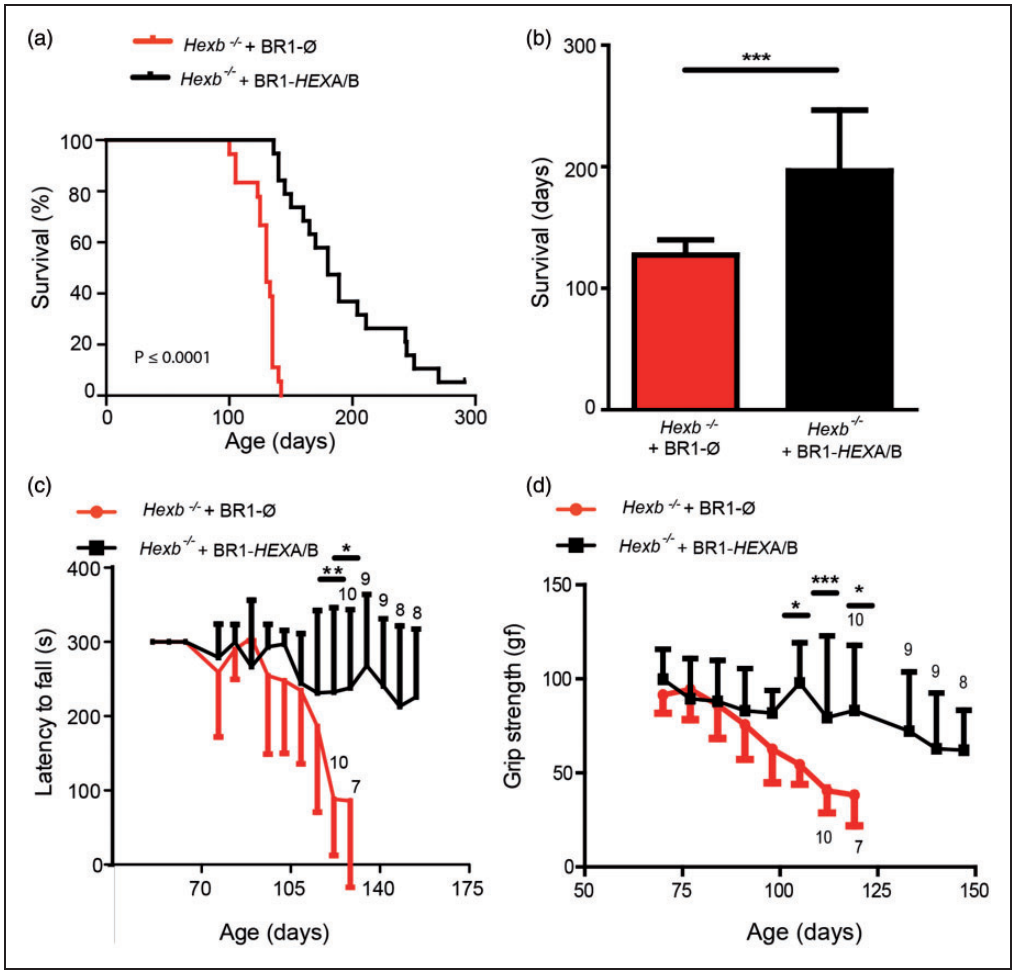

Figure 2. Transducing endothelial cells with AAV-BR1-CAG-*HEXA/B* improves survival and motor activity in $Hexb^{-/-}$ mice. $Hexb^{-/-}$ mice were treated 25–30 days after birth with AAV-BR1-CAG-*HEXA/B* or the control vector AAV-BR1-CAG-Ø (1.8×10^{11} gp/mouse) and monitored for up to 300 days. (a) Survival of $Hexb^{-/-}$ mice up to 300 days. Mice treated with AAV-BR1-*HEXA/B* survived significantly longer than the control group. At day 142, 15 out of 18 mice treated with AAV-BR1-*HEXA/B* survived whereas all animals in the group treated with AAV-BR1-CAG-Ø had died. Log-rank (Mantel-Cox) test showed a p value of < 0.0001. Control ($n = 18$), *HEXA/B* ($n = 19$) (b) Median survival in AAV-BR1-CAG-*HEXA/B* treated mice was 189 days in comparison to 130 days in the $Hexb^{-/-}$ control group. Data represent median ± SD and were analyzed by student t-test ($p < 0.0001$). Control ($n = 18$), *HEXA/B* ($n = 19$). (c) Latency to fall. Mice were placed on rotarod at a constant speed of 5 r/min for 5 min. The data at each time point are presented as mean ± SD. Control $Hexb^{-/-}$ mice performed poorly on the rotarod compared to the AAV-BR1-CAG-*HEXA/B*-treated group. $^{**}p < 0.01$; $^{*}p < 0.05$ (t test with Bonferroni correction for multiple testing). Sample sizes are indicated in the graph. (d) Grip strength of $Hexb^{-/-}$ control mice compared to $Hexb^{-/-}$ animals treated with the vectors AAV-BR1-CAG-*HEXA/B*. From the age of 99 days onwards, *HEXA/B* treated mice performed better than animals that received the control vector. $^{*}p < 0.05$; $^{***}p < 0.0001$ (t test with Bonferroni correction for multiple testing). The sample sizes are indicated in the graph.

more deposits in the cortex, striatum, and cerebellum than in the AAV-BR1-CAG-*HEXA/B*-treated group (Figure 3(a) and (b)). After extracting glycosphingolipids from brains of 110- to 120-day-old wild-type or heterozygote mice (summarized as $Hexb^{+/?}$ in Figure 3), AAV-BR1-CAG-*HEXA/B*-treated $Hexb^{-/-}$ mice, and AAV-BR1-CAG-Ø-treated $Hexb^{-/-}$ mice, we determined gangliosides by thin-layer chromatography (TLC). GM2 was quantified relative to sphingomyelins (SM) (Figure 3(c)). As expected, GM2 accumulated in $Hexb^{-/-}$ mice. AAV-BR1-CAG-*HEXA/B* treatment of $Hexb^{-/-}$ mice significantly reduced GM2 levels compared to the AAV-BR1-CAG-Ø-treated group. To further validate our results, GM2 and other sphingolipids were measured from the same groups of mice by mass spectrometry. Again, we observed a significant reduction in GM2 levels in the AAV-BR1-CAG-*HEXA/B*-treated group compared to the mice that received the control vector, as shown for GM2 (d36:1) (Figure 3(d)). Moreover, treatment of $Hexb^{-/-}$ mice with the vectors AAV-BR1-CAG-*HEXA/B* significantly reduced GA2 (d36:1) levels.

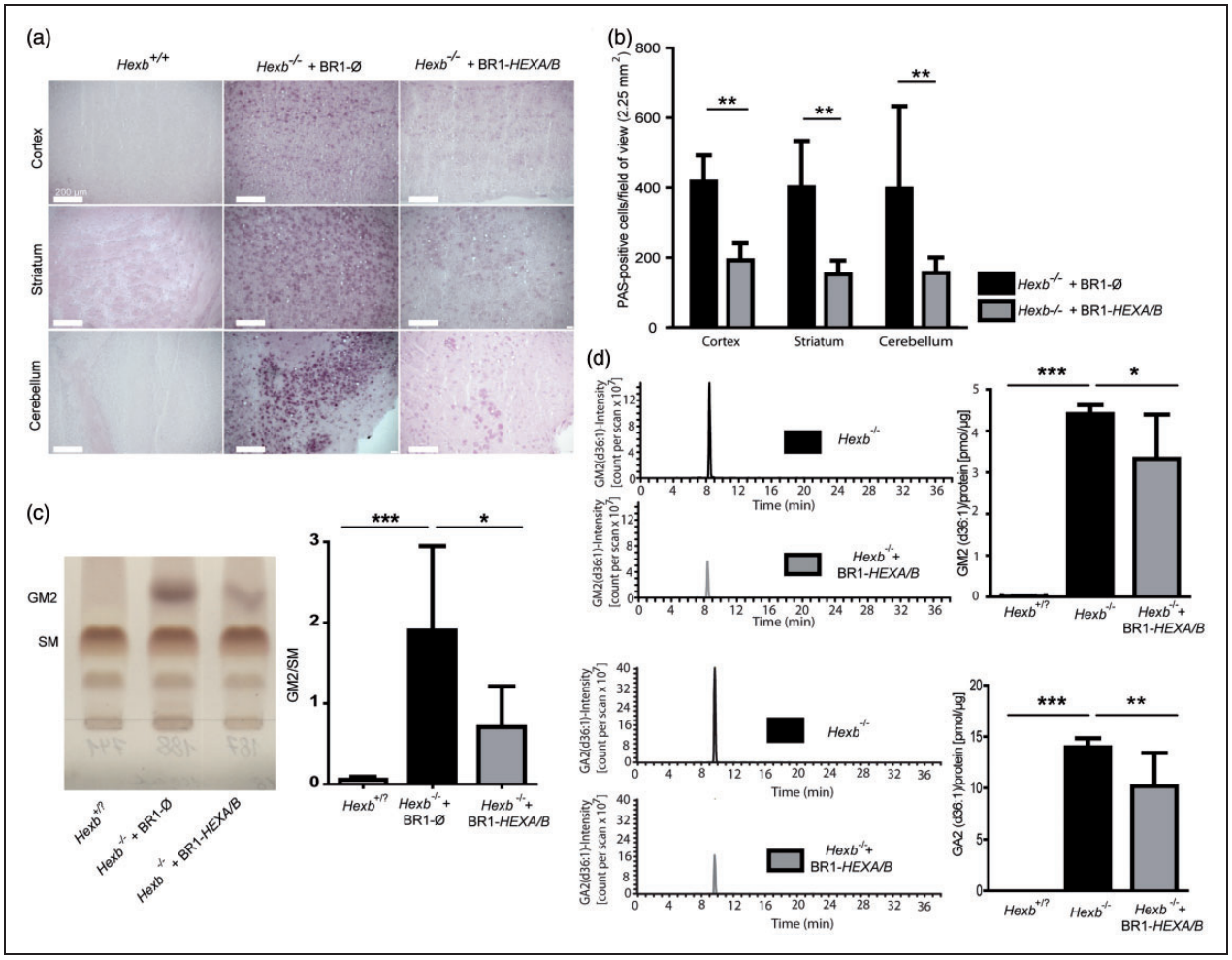

Figure 3. Transduction of brain endothelial cells with AAV-BR1-CAG-*HEXA/B* reduces ganglioside accumulation in $Hexb^{-/-}$ mice. (a) Periodic acid–Schiff (PAS) staining revealed glycospingolipid storage in 85–95 days old $Hexb^{-/-}$ mice but not in $Hexb^{+/+}$ and $Hexb^{+/-}$ controls (summarized as $Hexb^{+/?}$ in Figure 3). $Hexb^{-/-}$ mice were treated with AAV-BR1-CAG-*HEXA/B* or the control vector AAV-BR1-CAG-Ø at the age of 25–30 days. (b) Number of PAS-positive neurons in the cortex, striatum, and cerebellum of $Hexb^{-/-}$ mice treated with AAV-BR1-CAG-Ø or AAV-BR1-CAG-*HEXA/B*. There were significantly less PAS-positive neurons in the AAV-BR1-CAG-*HEXA/B*- than in the AAV-BR1-CAG-Ø-treated mice. Data are presented as mean ± SD and analyzed by two-way ANOVA (treatment, $F(1/27) = 41.43$, $p < 0.0001$; brain region and interaction were not significant). $^{**}p < 0.01$ (Bonferroni test, $n = 4$ mice per group). (c) Quantification of GM2 accumulation in $Hexb^{+/?}$ and $Hexb^{-/-}$ mice treated with AAV-BR1-CAG-*HEXA/B* or the control vector AAV-BR1-CAG-Ø at the age of 25–30 days. Brain extracts of 110- to 120-day-old mice were used for GM2 measurement by TLC. The right panel is a quantitative analysis of the TLC data. Results are presented as means ± SD and analyzed by one-way ANOVA ($F(2/14) = 9.683$, $p = 0.003$). $^{*}p < 0.05$, $^{**}p < 0.01$ (Bonferroni test, $n = 5$ mice per group). (d) Quantification of GM2(d36:1) and GA2(d36:1) accumulation via mass spectrometry in brain lysates of 110- to 120-day-old $Hexb^{+/?}$, $Hexb^{-/-}$ and $Hexb^{-/-}$ mice treated with the vectors AAV-BR1-CAG-*HEXA/B* at the age of 25–30 days. GM2(d36:1) and GA2(d36:1) accumulated in brains of $Hexb^{-/-}$ mice. AAV-BR1-CAG-*HEXA/B* treatment of $Hexb^{-/-}$ mice significantly reduced GM2 and GA2 levels compared to untreated $Hexb^{-/-}$ mice. $Hexb^{+/?}$ animals showed no accumulation of GM2 and GA2. Data are presented as means ± SD and analyzed by one-way ANOVA (GM2, $F(2/14) = 67.35$, $p < 0.0001$; GA2, $F(2/14) = 68.59$, $p < 0.0001$). $^{*}p < 0.05$; $^{***}p < 0.0001$ (Bonferroni test, $n = 5$ per group).

Expression of HEXA/B *reduces astrocytic activation*

Pathology in Sandhoff disease is typically associated with astrocyte activation, probably reflecting a neuroinflammatory response.[30] To investigate the effects of endothelial *HEXA/B* expression on the response of astrocytes in the brain of $Hexb^{-/-}$ mice, we injected either the control vector AAV-BR1-CAG-Ø or AAV-BR1-CAG-*HEXA/B* in mice at the age of 25–30 days. At the age of 85–95 days, the mice were sacrificed and brain sections were immunostained for GFAP, a marker of astrocytic activation. In various brain regions (cortex, striatum, and cerebellum), GFAP immunostaining was significantly reduced in $Hexb^{-/-}$

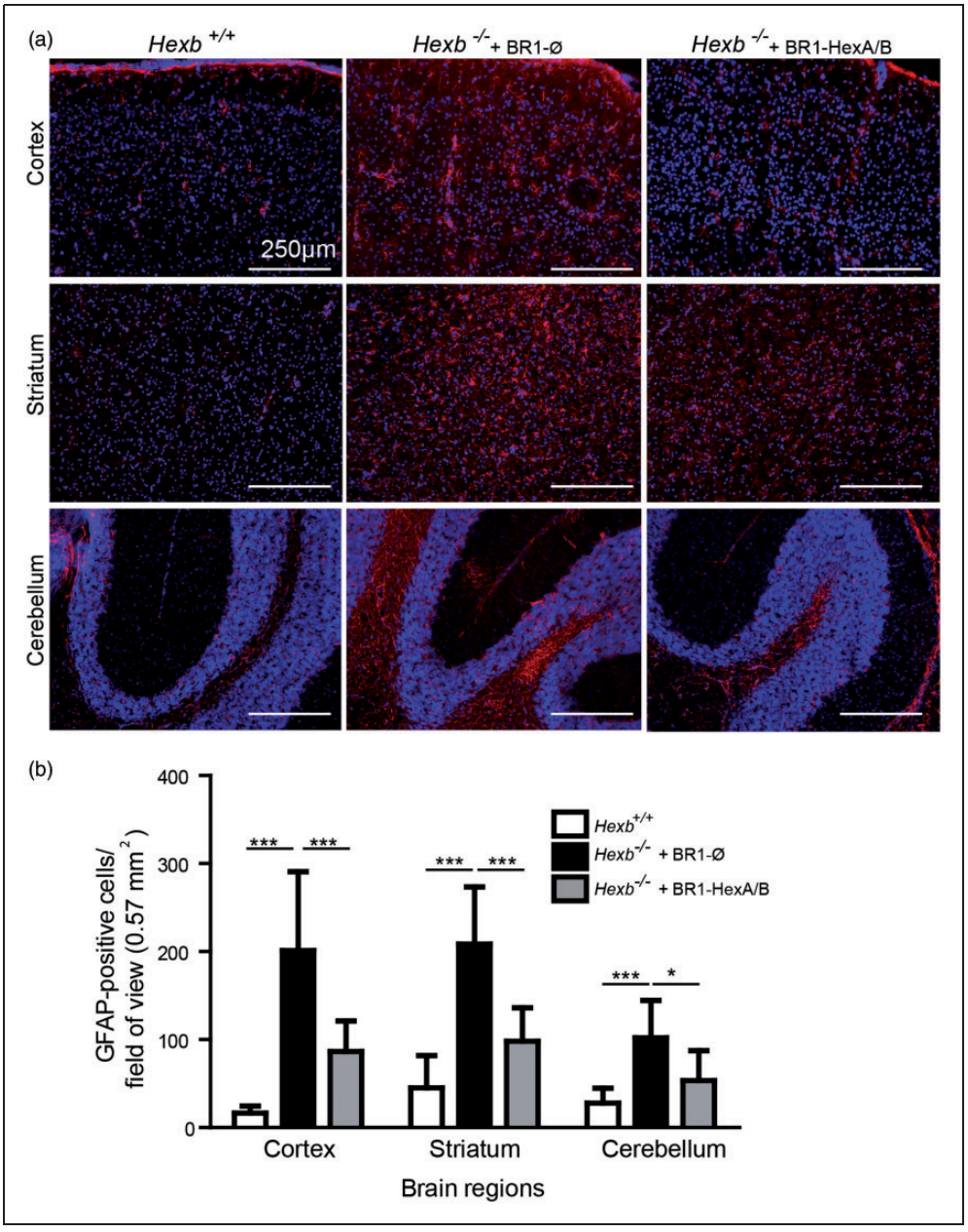

Figure 4. Transduction of endothelial cells with AAV-BR1-CAG-*HEXA/B* reduces astrocytic activation in $Hexb^{-/-}$ mice. (a) GFAP immunostaining of brain sections from $Hexb^{+/+}$ and $Hexb^{-/-}$ mice which were treated either with the vectors AAV-BR1-CAG-*HEXA/B* or AAV-BR1-CAG-Ø at the age of 25–30 days and were sacrificed at the age of 85–95 days indicated that endothelial *HEXA/B* expression blunted astrocytic activation in different brain regions. (b) Quantification of astrocytic activation by counting GFAP-positive cells in different brain regions. Data are means ± SD analyzed by one-way ANOVA (cortex, $F(2/29) = 28.02$, $p < 0.0001$; striatum, $F(2/29) = 29.55$, $p < 0.0001$; cerebellum, $F(2/23) = 11.08$, $p < 0.0005$), $^{*}p < 0.05$, $^{***}p < 0.0001$ (Bonferroni test, $n = 5$ mice per group).

mice treated with AAV-BR1-CAG-*HEXA/B* (Figure 4(a), right) compared to the $Hexb^{-/-}$ group that received the control vector (Figure 4(a), middle). Statistical evaluation of the number of GFAP-positive cells in the different brain regions indicated a significant reduction in astrocytic activation when mice were treated with the *HEXA/B*-expressing vectors (Figure 4(b)).

Discussion

In gangliosidoses, lipids accumulate in neurons and neurons subsequently die. This observation suggested that neurons are natural targets for gene therapy of these disorders. However, expression of *HEXA/HEXB* in neurons does not reflect the physiological situation,

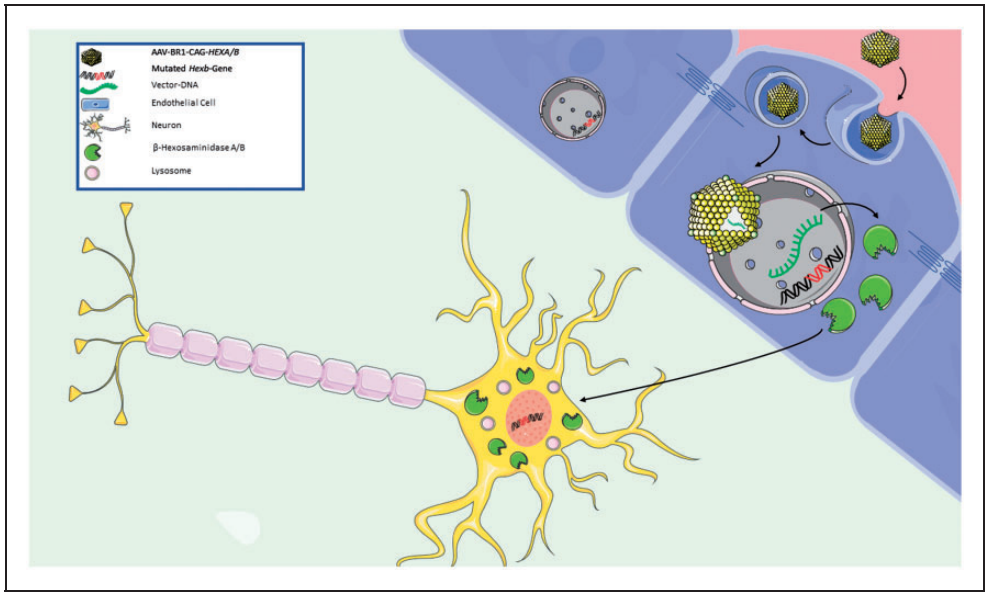

Figure 5. Schematic overview of the underlying concept. Intravenously injected AAV-BR1-CAG-*HEXA/B* vectors transduce brain endothelial cells. The vector DNA is transcribed, leading to the production of β-hexosaminidase which is released into the brain parenchyma. Although not shown in this study, neurons probably endocytose β-hexosaminidase, which enables the degradation of gangliosides and rescues the cells from neurodegeneration.

in which β-hexosaminidase is mainly expressed outside of neurons,[15,16] and, worryingly, has led to neuronal cell death in primates.[13] In a mouse model of amyotrophic lateral sclerosis, degenerating neurons expressed *Hexb*, supporting a detrimental role of *Hexb* expression in neurons.[31] Therefore, we tested the efficacy of non-neuronal expression of *HEXA*/*HEXB* in endothelial cells. After transduction, endothelial cells released β-hexosaminidase (Figure, 1(a)) and counteracted GM2 and GA2 accumulation in the brains of $Hexb^{-/-}$ mice (Figure 5). More importantly, endothelial targeting reduced signs of glial activation, improved neurological function, and prolonged survival of $Hexb^{-/-}$ mice. In summary, our data demonstrate that a cross-correction of neuronal *β*-hexosaminidase deficiency is possible and they also attest that under physiological conditions a similar mechanism may supply β-hexosaminidase to neurons. Mimicking the physiological cross-correction may increase the safety of the therapy in primates and humans.

A practical advantage of the new gene therapy reported here is the peripheral administration of AAV-BR1-CAG-*HEXA*/*B* by a single intravenous injection and the relatively low transduction in the liver. The latter will reduce the risk of insertional mutagenesis and hepatocellular carcinoma, which pose a potential risk in AAV-based therapies.[9]

Presently, the endothelium-targeted *HEXA*/*B* expression prolongs survival but does not cure experimental Sandhoff disease as other forms of gene therapy do.[8,10] The endothelium-targeted approach might be further improved by expressing a hybrid β-hexosaminidase subunit, such as *HEXM*, with a single vector instead of the *HEXA* and *HEXB,* which requires the transduction of target cells by two independent vectors.[32] To maximize therapeutic benefits, other studies have administered gene vectors to $Hexb^{-/-}$ mice in early life.[8,10] With AAV-BR1-CAG-*HEXA*/*B*, neonatal administration did not markedly enhance therapeutic effects. As AAV vectors mainly form episomes in the transduced cells, we speculate that postnatal angiogenesis[20] may have diluted the gene dose per cell. Administration of the vector at an age of about 14 days when endothelial cells reach a quiescent state in mice may solve this problem.

Subpopulations of brain endothelial cells highly express ribosomal protein transcripts,[33] indicating that they are well equipped for protein production in the brain. In addition, they are accessible from peripheral circulation. Thus, endothelium-targeted gene therapy may be applicable to other brain diseases, particularly those that are caused by endothelial dysfunction[22,34,35] or can be treated by cross-correction with secreted enzymes, such as Sandhoff disease.

Acknowledgements

We are grateful to Rolf Sprengel, University of Heidelberg Germany, for providing the plasmid p179 and to Jakob Körbelin and Martin Trepel, University Medical Center Hamburg-Eppendorf Germany, for providing the AAV-

BR1. We also thank Beate Lembrich, Frauke Spiecker, and Ines Stölting, Lübeck, Germany, for expert support.

Funding

The author(s) disclosed receipt of the following financial support for the research, authorship, and/or publication of this article: This work was funded by the German Research Foundation (DFG, SCHW416/9-1 to MS).

Declaration of conflicting interests

The author(s) declared no potential conflicts of interest with respect to the research, authorship, and/or publication of this article.

Authors' contribution

GD, MS, and HG designed the experiments; GD, HG, AO, and AP performed the experiments; GD, HG, AO, AP, and MS analyzed the data; and GD, HG, AO, AP, and MS wrote the manuscript.

Supplementary material

Supplementary information can be found at http://jcbfm.sagepub.com/content/by/supplemental-data.

ORCID iD

Markus Schwaninger https://orcid.org/0000-0002-4510-9718

References

1. Fuller M, Meikle PJ and Hopwood JJ. Epidemiology of lysosomal storage diseases: an overview. In: Mehta A, Beck M and Sunder-Plassmann G (eds) *Fabry disease: Perspectives from 5 years of FOS*. Oxford: PharmaGenetics, 2006, pp.9–20.
2. Neufeld EF. Enzyme replacement therapy – a brief history. In: Mehta ABM and Sunder-Plassmann G (eds) *Fabry disease: Perspectives from 5 years of FOS*. Oxford: Oxford PharmaGenesis, 2006.
3. Sandhoff K and Harzer K. Gangliosides and gangliosidoses: principles of molecular and metabolic pathogenesis. *J Neurosci* 2013; 33: 10195–10208.
4. Kitakaze K, Mizutani Y, Sugiyama E, et al. Protease-resistant modified human beta-hexosaminidase B ameliorates symptoms in GM2 gangliosidosis model. *J Clin Invest* 2016; 126: 1691–1703.
5. Tsuji D, Akeboshi H, Matsuoka K, et al. Highly phosphomannosylated enzyme replacement therapy for GM2 gangliosidosis. *Ann Neurol* 2011; 69: 691–701.
6. Cachon-Gonzalez MB, Wang SZ, McNair R, et al. Gene transfer corrects acute GM2 gangliosidosis–potential therapeutic contribution of perivascular enzyme flow. *Mol Ther* 2012; 20: 1489–1500.
7. Foust KD, Nurre E, Montgomery CL, et al. Intravascular AAV9 preferentially targets neonatal neurons and adult astrocytes. *Nat Biotechnol* 2009; 27: 59–65.
8. Walia JS, Altaleb N, Bello A, et al. Long-term correction of Sandhoff disease following intravenous delivery of rAAV9 to mouse neonates. *Mol Ther* 2015; 23: 414–422.
9. Nault JC, Datta S, Imbeaud S, et al. Recurrent AAV2-related insertional mutagenesis in human hepatocellular carcinomas. *Nat Genet* 2015; 47: 1187–1193.
10. Niemir N, Rouviere L, Besse A, et al. Intravenous administration of scAAV9-Hexb normalizes lifespan and prevents pathology in Sandhoff disease mice. *Hum Mol Genet* 2018; 27: 954–968.
11. Bradbury AM, Peterson TA, Gross AL, et al. AAV-mediated gene delivery attenuates neuroinflammation in feline Sandhoff disease. *Neuroscience* 2017; 340: 117–125.
12. Gray-Edwards HL, Randle AN, Maitland SA, et al. Adeno-Associated Virus Gene Therapy in a Sheep Model of Tay-Sachs Disease. *Human Gene Ther* 2018; 29: 312–326.
13. Golebiowski D, van der Bom IMJ, Kwon CS, et al. Direct intracranial injection of AAVrh8 encoding monkey beta-N-acetylhexosaminidase causes neurotoxicity in the primate brain. *Human Gene Ther* 2017; 28: 510–522.
14. Sango K, Yamanaka S, Hoffmann A, et al. Mouse models of Tay-Sachs and Sandhoff diseases differ in neurologic phenotype and ganglioside metabolism. *Nat Genet* 1995; 11: 170–176.
15. Hickman SE, Kingery ND, Ohsumi TK, et al. The microglial sensome revealed by direct RNA sequencing. *Nat Neurosci* 2013; 16: 1896–1905.
16. Saunders A, Macosko EZ, Wysoker A, et al. Molecular diversity and specializations among the cells of the adult mouse brain. *Cell* 2018; 174: 1015–1030 e1016.
17. Goebel HH. Morphology of the gangliosidoses. *Neuropediatrics* 1984; 15: 97–106.
18. Kyrkanides S, Brouxhon SM, Tallents RH, et al. Conditional expression of human beta-hexosaminidase in the neurons of Sandhoff disease rescues mice from neurodegeneration but not neuroinflammation. *J Neuroinflammation* 2012; 9: 186.
19. Batista L, Miller F, Clave C, et al. Induced secretion of beta-hexosaminidase by human brain endothelial cells: a novel approach in Sandhoff disease? *Neurobiol Dis* 2010; 37: 656–660.
20. Harb R, Whiteus C, Freitas C, et al. In vivo imaging of cerebral microvascular plasticity from birth to death. *J Cereb Blood Flow Metab* 2013; 33: 146–156.
21. Chen YH, Chang M and Davidson BL. Molecular signatures of disease brain endothelia provide new sites for CNS-directed enzyme therapy. *Nat Med* 2009; 15: 1215–1218.
22. Dogbevia GK, Tollner K, Korbelin J, et al. Gene therapy decreases seizures in a model of Incontinentia pigmenti. *Ann Neurol* 2017; 82: 93–104.
23. Korbelin J, Dogbevia G, Michelfelder S, et al. A brain microvasculature endothelial cell-specific viral vector with the potential to treat neurovascular and neurological diseases. *EMBO Mol Med* 2016; 8: 609–625.
24. Grimm D, Kay MA and Kleinschmidt JA. Helper virus-free, optically controllable, and two-plasmid-based

production of adeno-associated virus vectors of serotypes 1 to 6. *Mol Ther* 2003; 7: 839–850.
25. Xiao X, Li J, Samulski RJ. Production of high-titer recombinant adeno-associated virus vectors in the absence of helper adenovirus. *J Virol* 1998; 72: 2224–2232.
26. Ridder DA, Lang MF, Salinin S, et al. TAK1 in brain endothelial cells mediates fever and lethargy. *J Exp Med* 2011; 208: 2615–2623.
27. Huang Q, Zhou X, Liu D, et al. A new liquid chromatography/tandem mass spectrometry method for quantification of gangliosides in human plasma. *Anal Biochem* 2014; 455: 26–34.
28. Narvaez-Rivas M and Zhang Q. Comprehensive untargeted lipidomic analysis using core-shell C30 particle column and high field orbitrap mass spectrometer. *J Chromatogr A* 2016; 1440: 123–134.
29. Wendeler M and Sandhoff K. Hexosaminidase assays. *Glycoconjugate Journal* 2009; 26: 945–952.
30. Abo-Ouf H, Hooper AW, White EJ, et al. Deletion of tumor necrosis factor-alpha ameliorates neurodegeneration in Sandhoff disease mice. *Hum Mol Genet* 2013; 22: 3960–3975.
31. Lobsiger CS, Boillee S and Cleveland DW. Toxicity from different SOD1 mutants dysregulates the complement system and the neuronal regenerative response in ALS motor neurons. *Proc Natl Acad Sci U S A* 2007; 104: 7319–7326.
32. Tropak MB, Yonekawa S, Karumuthil-Melethil S, et al. Construction of a hybrid beta-hexosaminidase subunit capable of forming stable homodimers that hydrolyze GM2 ganglioside in vivo. *Mol Ther Meth Clin Dev* 2016; 3: 15057.
33. Vanlandewijck M, He L, Mae MA, et al. A molecular atlas of cell types and zonation in the brain vasculature. *Nature* 2018; 554: 475–480. 2018/02/15.
34. Tang M, Gao G, Rueda CB, et al. Brain microvasculature defects and Glut1 deficiency syndrome averted by early repletion of the glucose transporter-1 protein. *Nat Commun* 2017; 8: 14152.
35. Vatine GD, Al-Ahmad A, Barriga BK, et al. Modeling psychomotor retardation using iPSCs from MCT8-deficient patients indicates a prominent role for the blood-brain barrier. *Cell Stem Cell* 2017; 20: 831–843 e835.